Physica A 401 (2014) 182–200

Contents lists available at ScienceDirect

Physica A

journal homepage: www.elsevier.com/locate/physa

Pricing of range accrual swap in the quantum finance Libor Market Model

Belal E. Baaquie [a,b], Xin Du [a,*], Pan Tang [c], Yang Cao [a]

[a] Department of Physics, National University of Singapore, 2 Science Drive 3, Singapore 117542, Singapore

[b] Risk Management Institute, National University of Singapore, Singapore

[c] Department of Finance, School of Economics and Management, Southeast University, Nanjing, Jiangsu 210096, China

HIGHLIGHTS

- The range accrual swap is modelled in the framework of Quantum Finance and the approximate price is obtained using an expansion in the Libor volatility.
- The price of accrual swap is numerically analysed by generating daily sample values of a two dimension Gaussian quantum field.
- The Monte Carlo simulation method is used to study the nonlinear domain of the model and determine the range of validity of the approximate formula.

ARTICLE INFO

Article history:
Received 27 September 2013
Received in revised form 12 November 2013
Available online 28 January 2014

Keywords:
Quantum finance
Range accrual swap
Monte Carlo simulation

ABSTRACT

We study the range accrual swap in the quantum finance formulation of the Libor Market Model (LMM). It is shown that the formulation can exactly price the path dependent instrument. An approximate price is obtained as an expansion in the volatility of Libor. The Monte Carlo simulation method is used to study the nonlinear domain of the model and determine the range of validity of the approximate formula. The price of accrual swap is analyzed by generating daily sample values by simulating a two dimension Gaussian quantum field.

1. Introduction

Range accrual swap is a type of a derivative product that is similar to normal interest rate swap. The investor may have a view that the market is or is not very volatile and that consequently some index will or will not stay within a predefined range. The range accrual index could be an interest rate, an FX rate or a commodity price. The investor makes an additional profit if the view taken is correct and loses money otherwise. The range accrual can also serve to hedge risks since the payments are based on daily observations and not on a pre-fixed rate.

The interest range accrual swap is one of the most popular non-vanilla interest rate derivatives; more than USD 160 billion of range accrual indexed on interest rates have been sold since 2004, and the total volumes have been increasing rapidly in the last few years. The present work investigates the range accrual swap based on the behavior of the 3-month Libor.

The range accrual for interest rates has been studied in many books and articles, such as Navatte and Quittard-Pinon [1], Nunes [2] using the Gaussian HJM (Heath–Jarrow–Morton) framework, Damiano Brigo and Fabio Mercurio using the BGM-

* Corresponding author. Tel.: +65 96458390.
E-mail addresses: phybeb@nus.edu.sg (B.E. Baaquie), duxin.nus@gmail.com (X. Du), pantangnus@gmail.com (P. Tang), yangcao@nus.edu.sg (Y. Cao).

0378-4371/$ – see front matter
http://dx.doi.org/10.1016/j.physa.2014.01.042

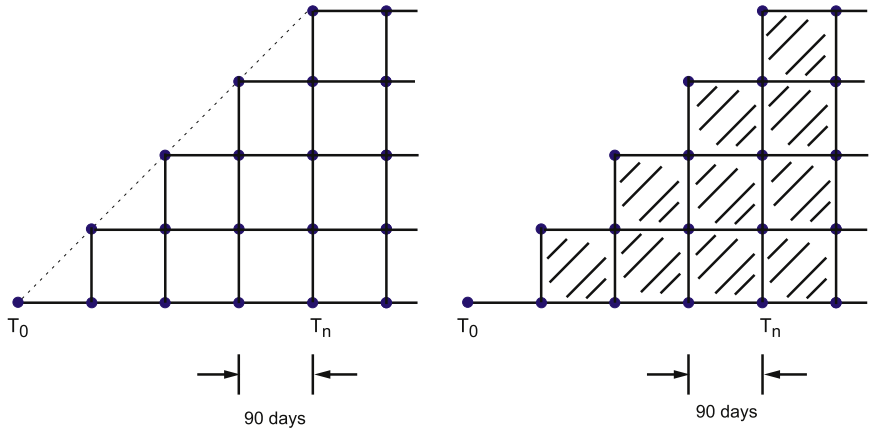

Fig. 1. The Libor lattice defined by $L(T_n, T_m)$. The shaded portion shows the time dependence of the Libor rates for the Libor lattice.

Jamshidian formulation of LMM [3] and Yoon and Jang [4] with jump risk. The quantum finance formulation of the Libor Market Model has been studied in Ref. [5].

Quantum field theory has been applied to many *classical problems*; two famous examples are (a) the solution of classical phase transitions by Wilson and which led to his physics Nobel Prize in 1982 [6] and (b) the complete classification of knots and links in three dimensions by Witten, for which he was awarded the Fields Medal in 1989 [7]. These examples show that the mathematics of quantum mechanics extends far beyond not only quantum systems but instead can be applied to a wide variety of phenomena, including even the social sciences [8]. The formalism of quantum finance has been developed in this spirit and is based on the application of *quantum mathematics* to finance [9,10]. In particular, interest rate models in quantum finance are based on the mathematics of a two-dimensional Euclidean quantum field.

This paper is organized as follows. Section 2 briefly reviews LMM in quantum finance. In Sections 3 and 4 the range accrual swap is defined in the mathematical framework of the quantum LMM. In Section 5 we derive an analytical approximate formula for the price of the range accrual swap. In Sections 6, 7, we carry out a Monte Carlo simulation to evaluate the price of the range accrual swap. In particular, we compare the approximate analytical expression for the range accrual swap with simulation results. We draw some conclusions in the final Section 8.

2. Libor market model

The forward interest rate, denoted by $f(t, x)$, is the interest rate fixed at time t for an overnight loan at future time $x > t$. Both the bond market and interest paid on cash deposits are determined by $f(t, x)$. The standard industry bench mark is given by two models, namely the HJM model that is used to price bonds and the BGM-Jamshidian model that quantifies the interest rate paid on cash deposits.

To mathematically define the industry bench-mark models let $R(t)$ be Gaussian white noise with correlators given by

$$E[R(t)] = 0; \qquad E[R(t)R(t')] = \delta(t - t').$$

The HJM model is a linear model defined by

$$\frac{\partial f(t, x)}{\partial t} = \alpha(t, x) + \sigma(t, x)R(t) \tag{1}$$

where $\alpha(t, x)$, $\sigma(t, x)$ are deterministic functions.

The Libor interest rate $L(t, T_n)$ is a simple interest rate, fixed at time t, for making a cash deposit at future time T_n for a duration of time ℓ, called the tenor of the deposit. Simple interest Libor rates $L(t, T_n)$ are defined on the Libor future time lattice defined by $T_n = n\ell$, where ℓ is Libor tenor. The Libor lattice is shown in Fig. 1; for fixed tenor ℓ Libor rates are only defined on the Libor interval $[T_n, T_{n+1}]$; the shaded portion in Fig. 1 shows all the Libor rates that exist for the Libor lattice.

In terms of Libor forward interest rates $L(t, T_n)$ is given by

$$1 + \ell L(t, T_n) = \mathrm{e}^{\int_{T_n}^{T_{n+1}} \mathrm{d}x f(t,x)}. \tag{2}$$

BGM-Jamshidian formulation of LMM is defined by

$$\frac{1}{L(t, T_n)} \frac{\partial L(t, T_n)}{\partial t} = \xi_n(t) + \gamma_n(t)R(t) \tag{3}$$

where $\gamma_n(t)$ is a deterministic function; $\xi_n(t)$ is a function of Libor rates $L(t, T_n)$ and hence makes the model nonlinear.

The quantum finance formulation of the Libor Market Model (LMM) was first obtained by Baaquie [5] based on generalizing the one dimensional random noise $R(t)$ to a two dimensional classical stochastic field $A(t, x)$; from a mathematical point of view, $A(t, x)$ is a two dimensional Euclidean Gaussian quantum field. Libor forward interest rates $f_L(t, x)$, are in principle equal to $f(t, x)$ but written with a subscript L to differentiate it from the HJM forward interest rates, is defined for both calendar time t and future time x. The Libor forward rate in quantum finance approach is given by the following:

$$\frac{\partial f_L(t,x)}{\partial t} = \mu(t,x) + \upsilon(t,x)A(t,x) \tag{4}$$

where the drift $\mu(t, x)$ and volatility $\upsilon(t, x)$ both depend on the $f_L(t, x)$ making the model nonlinear. The correlation of the Gaussian field $A(t, x)$ is

$$E[A(t,x)A(t',x')] = \delta(t-t')D(x,x';t) \tag{5}$$

where $D(x, x'; t)$ is the propagator.

The quantum finance formulation of LMM $L(t, T_n)$ is given by

$$\frac{1}{L(t,T_n)}\frac{\partial L(t,T_n)}{\partial t} = \xi(t,x) + \int_{T_n}^{T_{n+1}} \gamma(t,x)A(t,x) \tag{6}$$

where $\gamma(t, x)$ is the *deterministic volatility*. It is due to the deterministic volatility γ that the LMM is well defined.

Baaquie [5] defined the logarithmic field $\phi(t, x)$ that drives Libor interest rates as follows:

$$\ell L(t,T_n) = \mathrm{e}^{\int_{T_n}^{T_{n+1}} \phi(t,x)\mathrm{d}x} \equiv \mathrm{e}^{\phi_n(t)} \tag{7}$$

$\phi(t, x)$ is mathematically equivalent to a two-dimensional Euclidean quantum field and has dimensions of 1/time; the time evolution of $\phi(t, x)$ is given by

$$\frac{\partial\phi(t,x)}{\partial t} = -\frac{\Lambda_n(t,x)}{2} + \rho_n(t,x) + \gamma(t,x)A(t,x); \qquad T_n < x \le T_{n+1}$$

$$\Lambda_n(t,x) = \int_{T_n}^{T_{n+1}} \mathrm{d}x'\gamma(t,x)D(x,x';t)\gamma(t,x').$$

The total drift has a deterministic piece $\Lambda_n(t, x)$ and a stochastic term $\rho_n(t, x)$.

To find its present value, all future cash flows need to be discounted by a 'numeraire'—based on the prevailing interest rates and encoding the time value of money. The forward bond numeraire is given by $B(t, T_{l+1})$; for any Libor based financial instrument $\mathcal{F}[L, t]$ the martingale condition states that

$$\frac{\mathcal{F}[L,T_0]}{B(T_0,T_{l+1})} = E_l\left[\frac{\mathcal{F}[L,T_n]}{B(T_n,T_{l+1})}\right]. \tag{8}$$

The subscript I is the symbol for the expectation value, namely $E_l[..]$, to indicate that the expectation value is being taken over a stochastic process that has a martingale evolution with respect to the numeraire $B(t, T_{l+1})$.

The drift $\rho_n(t, x)$ of the LMM is obtained by requiring that the time evolution of all Libor rates follow a martingale process with respect to the numeraire $B(t, T_{l+1})$; imposing the martingale condition derived in Appendix A and yields the following drift [5]

$$\rho_n(t,x) = \left\{\begin{array}{ll} \displaystyle\sum_{m=l+1}^{n} \frac{\mathrm{e}^{\phi_m(t)}}{1+\mathrm{e}^{\phi_m(t)}}\Lambda_m(t,x) & n > l \\ 0 & n = l \\ \displaystyle-\sum_{m=n+1}^{l} \frac{\mathrm{e}^{\phi_m(t)}}{1+\mathrm{e}^{\phi_m(t)}}\Lambda_m(t,x) & n < l \end{array}\right\} : \; T_n \le x < T_{n+1}. \tag{9}$$

Note that Eq. (9) defines the drift $\rho_n(t, x)$ for x in the Libor lattice that $T_n < x \le T_{n+1}$ for some n; as x takes values in different parts of the Libor lattice, the drift $\rho_n(t, x)$ also changes.

2.1. Lagrangian and path integral for $\phi(t, x)$

The quantum field theory of the stochastic field driving the interest rates is defined by a functional integral over all configurations of $A(t, x)$. The partition function is given by

$$Z = \int DA\mathrm{e}^{S[A]}. \tag{10}$$

Fig. 2. Diagram representing cash flows, at some future time, for a swap.

The Lagrangian and action for the Gaussian quantum field $A(t, x)$ are given by the following:

$$S[A] = \int_0^\infty \mathrm{d}t \int_t^\infty \mathrm{d}x \mathcal{L}[A]; \quad \mathcal{L}[A] = -\frac{1}{2} A(t, x) D^{-1}(x, x'; t) A(t, x'). \tag{11}$$

All financial instruments of the interest rates are obtained by performing a path integral over the (fluctuating) two dimensional quantum field $A(t, x)$. The expectation value for an instrument, say $Q[A]$, is denoted by $E[Q[A]]$ and is defined by the functional average over all values of $A(t, x)$, weighted by the probability measure e^S/Z, discussed in Baaquie [5]. Hence

$$E[Q[A]] = \frac{1}{Z} \int DAQ[A] \mathrm{e}^{S[A]}. \tag{12}$$

The quantum field theory of the forward interest rates is given by

$$Z[h(t, x)] = E[\mathrm{e}^{\int_{t_0}^\infty \int_0^\infty h(t,x) A(t,x) \mathrm{d}x}].$$

For a quadratic Lagrangian, such as the one given in Eq. (11), the generating function is obtained by performing the Gaussian integrations and yields

$$\begin{aligned} Z[h(t, x)] &= \frac{1}{Z} \int DA \mathrm{e}^S \mathrm{e}^{\int_{t_0}^\infty \mathrm{d}t \int_0^\infty h(t,x) A(t,x) \mathrm{d}x} \\ &= \exp\left\{ \frac{1}{2} \int_{t_0}^\infty \mathrm{d}t \int_0^\infty \mathrm{d}x \mathrm{d}x' h(t, x) D(x, x'; t) h(t, x') \right\}. \end{aligned} \tag{13}$$

The correlators of the $A(t, x)$ quantum field are given by

$$E[A(t, x)] = 0 \tag{14}$$

$$\begin{aligned} E[A(t, x) A(t', x')] &= \frac{1}{Z} \int DA \mathrm{e}^{S[A]} A(t, x) A(t', x') \\ &= \delta(t - t') D(x, x'; t). \end{aligned} \tag{15}$$

The numerical simulation of $A(t, x)$ is discussed in Appendix B.

2.2. Interest rate swaps

An interest rate swap is an agreement made today, to exchange two streams of cash flows at some future time. It is contracted between two parties in which one party A pays a fixed interest rate R_S and receives floating fixed by Libor (at the future date) whereas the other party B pays a floating Libor and receives fixed; Fig. 2 schematically shows cash flows for a swap at some future time.

Consider a swaplet that receives a single floating payment and pays at a fixed rate R_S; the swaplet matures at time T_n and the floating rate is fixed by the value of the 90-day Libor, namely Libor $L(T_n, T_n)$; both the floating and fixed rates cash flows take place in *arrears*, at time T_{n+1}. For a sum of amount V, the value of the swaplet, at present time T_0, is equal to the future cash flows—discounted by bond $B(T_0, T_{n+1})$ to present time and T_0 and is given by the following [5]:

$$\mathrm{Swaplet}_L(T_0, R_s) = \ell V B(T_0, T_{n+1}) \big[L(T_0, T_n) - R_s \big]. \tag{16}$$

A swap consists of a portfolio of swaplets, starting at Libor time T_0; payments are made at fixed times $T_n = T_0 + n\ell$, with $n = 1, 2, \ldots, N - 1$; the first payment is made at T_1 and the last payment at T_N. The value at time T_0 of the floating rate receiver Swap_L and fixed rate receiver Swap_R is

$$\mathrm{Swap}_L(T_0, R_s) = \ell V \sum_{n=0}^{N-1} B(T_0, T_{n+1}) [L(T_0, T_n) - R_s]$$

$$\mathrm{Swap}_R(T_0, R_s) = \ell V \sum_{n=0}^{N-1} B(T_0, T_{n+1}) [R_s - L(T_0, T_n)]$$

$$\mathrm{Swap}_L(T_0, R_s) + \mathrm{Swap}_R(T_0, R_s) = 0.$$

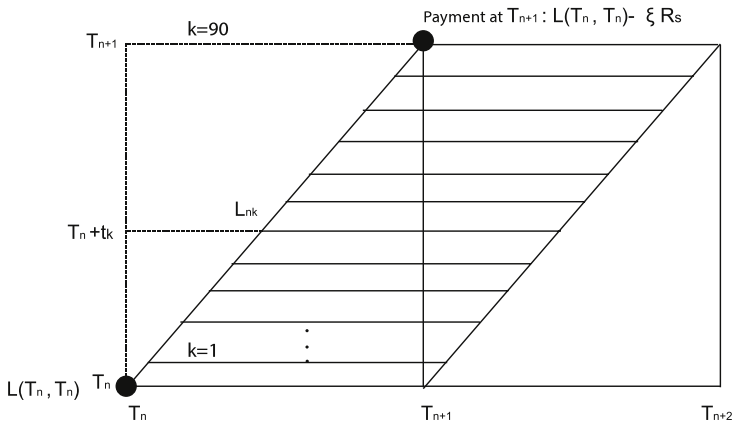

Fig. 3. The 90-day Libor rates for one payment period.

The par value $R_p(T_0)$ is defined to make the initial values equal for floating rate receiver Swap_L and fixed rate receiver Swap_R; hence

$$\text{Swap}_L(T_0, R_p(T_0)) = 0 = \text{Swap}_R(T_0, R_p(T_0)).$$

3. Range accrual swap

In a typical interest rate range accrual swap, the fixed rate R_S accrues *contingent* on a *pre-selected* Libor rate being within a *pre-fixed* range $[a, b]$ during a stipulated period preceding the payment. At payment date, the payment fraction is ξR_S where $\xi = \frac{\kappa}{M}$ and κ is the number of days that the pre-selected Libor was in the range for the payment period and M is the payment period of the individual swaplets. In this paper, the payments are made every $M = 90$ days and the 90-day Libor rate is tracked during this period to see how many days it was within the pre-specified range $[a, b]$.

Consider Fig. 3, where a single 90-day payment period is shown—from calendar time T_n to the next payment time T_{n+1}. The Libor for the swaplet, namely $L(T_n, T_n)$ is fixed at time T_n; however, unlike a normal swap for which the fixed rates are always R_S, for the accrual case, it is only fixed at the payment date, namely at time T_{n+1}.

The 90-day Libor at calendar time $T_n + t_k$, namely L_{nk}, is defined by

$$1 + \ell L_{nk} \equiv \exp\left\{\int_{T_n+t_k}^{T_{n+1}+t_k} \mathrm{d}x f(T_n + t_k, x)\right\} \tag{17}$$

with the unit function given by

$$1_{a<z<b} = \begin{cases} 1 & z \in [a, b] \\ 0 & \text{otherwise.} \end{cases}$$

The horizontal lines indicate the 90-day Libor L_{nk} for calendar time $T_n + t_k$. The value of the 90-day Libor is observed every day. In this way, it is determined for how many days κ was the 90-day Libor L_{nk} in the pre-fixed range. After 90 days, the rate for payment at time T_{n+1} is fixed to be $\xi R_S = \frac{\kappa}{M} \cdot R_S$ and the floating and 'fixed' cash flows are equal to $L(T_n, T_n) - \xi R_S$, as shown in Fig. 3.

The stochastic cash-flow at calendar time T_{n+1} defines the range accrual swaplet as the following:

$$\text{Swaplet}_A(T_n, T_n; a, b) = \ell VB(T_n, T_{n+1})\Big[L(T_n, T_n) - \frac{R_s}{M}\sum_{k=1}^{M} 1_{a<L_{nk}<b}\Big]. \tag{18}$$

The accrual time is defined for the 90-day Libor by the following:

$$\ell = 90\epsilon; \qquad t_k = k\epsilon; \quad \epsilon = 1 \text{ day}; \ k = 1, 2, \ldots, 90.$$

The bond $B(T_0, T_{n+1})$ in Fig. 4, expressed in terms of Libor rates, is given by

$$B(T_0, T_{n+1}) = \exp\left\{-\int_{T_0}^{T_{n+1}} \mathrm{d}x f_L(T_0, x)\right\} = \prod_{i=0}^{n} \frac{1}{1 + \ell L(T_0, T_i)}. \tag{19}$$

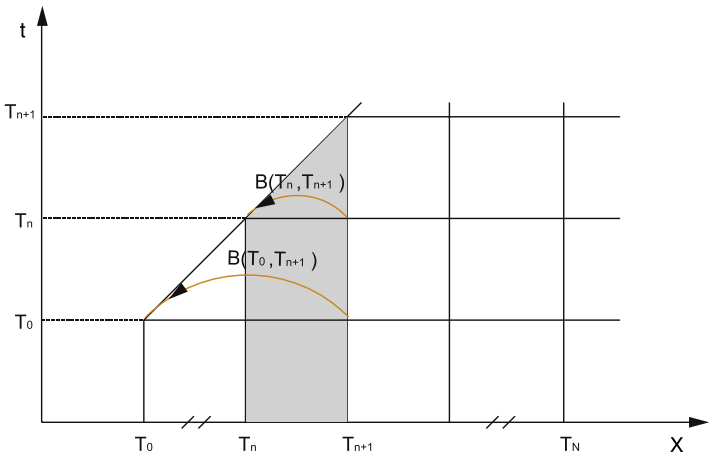

Fig. 4. The bond numeraire $B(T_n, T_{n+1})$ used for discounting price. The shaded area is the time interval.

For the swap accrual, the discounted value of each swaplet is evaluated separately; hence we can use a 'rolling' numeraire, choosing a numeraire tailored to simplify the calculation of each swaplet. The discounted price of a swaplet, using the numeraire $B(T_n, T_{I+1})$, is a martingale and yields, from Eqs. (8) and (18), that the swaplet price at present time T_0 is given by

$$\begin{aligned}\frac{\text{Swaplet}_A(T_0, T_n; a, b)}{B(T_0, T_{I+1})} &= \ell V E_I\left[\frac{\text{Swaplet}_A(T_n, T_n; a, b)}{B(T_n, T_{I+1})}\right] \\ &= \ell V E_I\left[\frac{B(T_n, T_{n+1})}{B(T_n, T_{I+1})}\left\{L(T_n, T_n) - \frac{R_s}{M}\sum_{k=1}^{M} 1_{a<L_{nk}<b}\right\}\right]. \end{aligned} \tag{20}$$

Using the numeraire $B(T_n, T_{n+1})$ for discounting, namely taking $I = n$, yields the following accrual swaplet price

$$\frac{\text{Swaplet}_A(T_0, T_n; a, b)}{B(T_0, T_{n+1})} = \ell V E_n\left[L(T_n, T_n) - \frac{R_s}{M}\sum_{k=1}^{M} 1_{a<L_{nk}<b}\right]. \tag{21}$$

Since

$$E_n[L(T_n, T_n)] = E_n\left[\frac{B(T_n, T_{n+1}) - B(T_n, T_n)}{\ell B(T_n, T_{n+1})}\right] = L(T_0, T_n), \tag{22}$$

the accrual swaplet, from Eqs. (20) and (22), is given by

$$\text{Swaplet}_A(T_0, T_n; a, b) = \ell V B(T_0, T_{n+1})\left\{L(T_0, T_n) - \frac{R_s}{M}\sum_{k=1}^{M} E_n[1_{a<L_{nk}<b}]\right\}.$$

The main difference from a normal swaplet is the calculation of the accrual part $E_n[1_{a<L_{nk}<b}]$, which is expectation value of the 90-day Libor L_{nk} being in the range at kth day, with the expectation value being performed for the $B(t, T_{n+1})$ numeraire.

If the future fixed payments are deterministic, as is the case for the usual swaplet for which the fixed payment is R_S, we recover the result for the swaplet given in Eq. (16), namely

$$\text{Swaplet}_L(T_0, R_s) = \ell V B(T_0, T_{n+1})\big[L(T_0, T_n) - R_s\big].$$

The Libor range accrual swap is given by the sum of swaplets for payments at different future calendar times T_n and yields

$$\text{Swap}_A(T_0, T_N; a, b) = \sum_{n=0}^{N-1} \text{Swaplet}_A(T_0, T_n; a, b). \tag{23}$$

Note that unlike a normal Swaplet(T_0, R_S), which has a deterministic value at time T_0 given by $\ell V B(T_0, T_{n+1})0$ $\big[L(T_0, T_n) - R_s\big]$, the range accrual Swaplet$_A(T_0, T_0; a, b)$ has a stochastic value, since the payment is only fixed at time T_1 and is given by $\ell V B(T_0, T_1)\big[L(T_0, T_1) - \xi R_s\big]$.

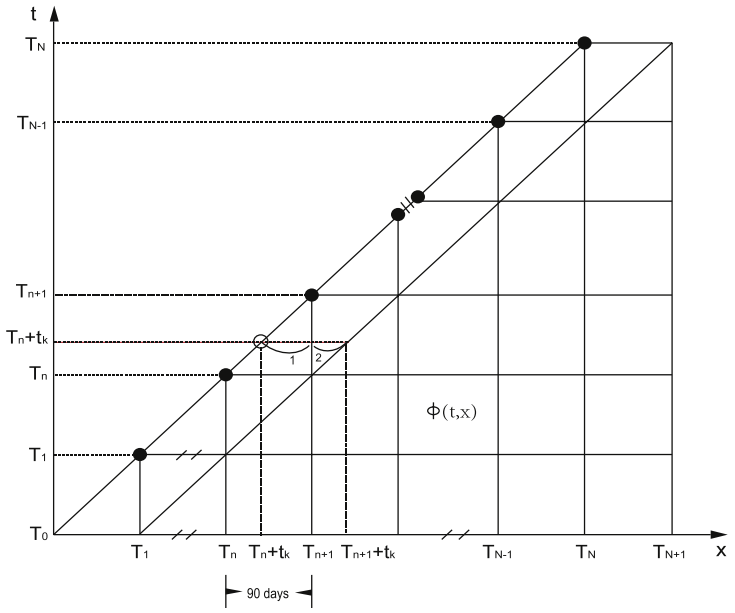

Fig. 5. The payoff function of Libor rate accrual swap; the value for $\phi(t, x)$ is required for the entire trapezoid domain.

3.1. Rang accrual swap payoff function

Fig. 5 shows the *payoff function* of the range accrual swap $\text{Swap}_A(T_0, T_N; a, b)$. Each black dot in the figure represents a 90-day Libor $L(T_n, T_m)$; the diagonal on the edge is the line along which calendar time is equal to future time. All the payments for each swaplet is made at one of the black dots on the diagonal line.

The line parallel to the edge diagonal indicates the 90-day Libor that are observed daily to determine how many days the 90-day Libor was in the pre-specified range $[a, b]$. The payoff function has a closure at future calendar time T_N: the last accrual swaplet $\text{Swaplet}_A(T_0, T_{N-1}; a, b)$ is exercised at time T_{N-1} with the final payments made at T_N.

The 90-day Libor L_{nk} being observed is indicated in Fig. 5 by the horizontal line with a circle; for time $T_n + t_k$, the figure shows that the 90-day Libor L_{nk} consists of a piece labeled 1 that starts at the diagonal edge, and then crosses the Libor lattice at future time T_{n+1}, with the piece labeled 2 being the remaining part of the 90-day Libor.

For pricing the range accrual swap, the values of the log-Libor field $\phi(t, x)$ have to be determined for every point in the entire trapezoid. This will be more clear in Section 6 where the simulation of the field $\phi(t, x)$ is carried out for pricing the accrual swap.

4. Extension of Libor drift

In terms of the log-Libor field, Libor L_{nk} defined in Eq. (17) is given as follows:

$$\ell L_{nk} \equiv \ell L(T_n + t_k, T_n + t_k) = \exp\left\{\int_{T_n+t_k}^{T_{n+1}+t_k} \mathrm{d}x\, \phi(T_n + t_k, x)\right\}. \tag{24}$$

Note that future time for L_{nk} does not lie in a Libor lattice, as given in Fig. 1, since it crosses the Libor lattice at time T_{n+1}—as shown in Fig. 5. At future time $T_n + t_k$, all the Libor rates for the full Libor lattice interval $[T_n, T_{n+1}]$ no longer exist since the Libor rates for $x < T_n + t_k$ have expired.

As it stands, the Libor Market Model is only defined for future time x lying in a Libor lattice $[T_m, T_{m+1}]$, where time $T_m > t$ is in the future to calendar time t; in particular, the drift in Libor Market Model is only defined for $\phi(t, x)$ with $T_n < x \leq T_{n+1}$. Comparing Figs. 1 and 6 shows that the field $\phi(t, x)$ needs to be defined in the wedge on the diagonal that does not have any Libor rates on the Libor lattice.

Hence, the drift given in Eq. (9) for the quantum formulation of LMM has to be extended for defining the evolution of $\phi(t, x)$ for x in the interval $[T_n + t_k, T_{n+1}]$. For the rolling numeraire, we take $I = n$ in the numeraire $B(t, T_{I+1})$; from Eq. (9), the stochastic drift $\rho_n(t, x)$ of the Libor rate for $T_n \leq x < T_{n+1}$ is zero and is non-zero for $T_{n+1} \leq x < T_{n+2}$. Hence

$$\rho_n(t, x) = \begin{cases} 0 & x \in [T_n, T_{n+1}] \\ \neq 0 & x \in [T_{n+1}, T_{n+2}]. \end{cases}$$

The stochastic drift for the range of $T_n \leq x < T_{n+2}$ is shown in Fig. 7.

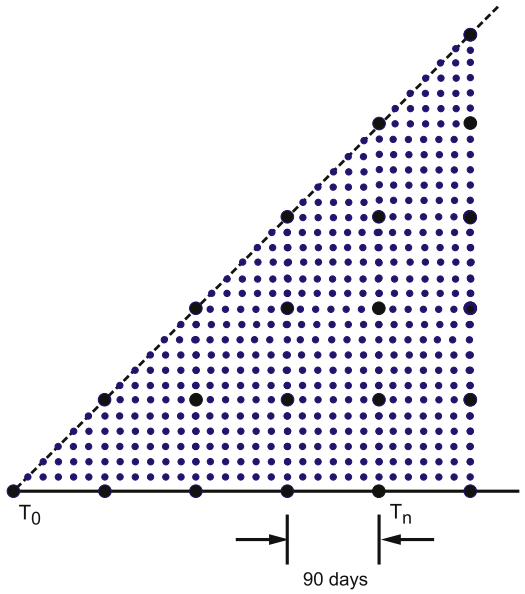

Fig. 6. The domain for $\phi(t, x)$ required for pricing the range accrual swap.

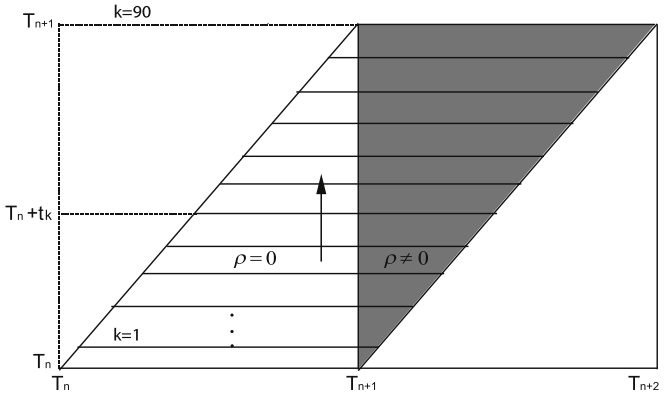

Fig. 7. The stochastic drift for Libor L_{nk} that crosses the Libor lattice at time T_{n+1}.

For the range of future time $T_n + t_k \leq x < T_{n+1}$, it follows from the discussion above that the stochastic drift $\rho_n(t, x)$ is zero. Hence, to extend the LMM so that it can price instruments such as the range accrual swap, we need to define the *deterministic drift* $\Lambda_n(t, x)$ for $T_n + t_k \leq x < T_{n+1}$.

Since $T_n + t_k$ does not lie on the Libor lattice, we extend the definition of deterministic drift $\Lambda_n(t, x)$ by cutting off the lower limit of the integration (that defines the deterministic drift) to a lower limit of $T_n + t_k$.

We consequently obtain the evolution equation for $\phi(t, x)$ in the following two parts, and which is shown in Fig. 7.

$$\begin{aligned}
&\text{I} : T_n + t_k \leq x < T_{n+1} \\
&\frac{\partial \phi(t,x)}{\partial t} = -\frac{\Lambda^{(1)}(t,x)}{2} + \rho_1(t,x) + \gamma(t,x)A(t,x) \\
&\Lambda^{(1)}(t,x) \equiv \int_{T_n+t_k}^{T_{n+1}} \mathrm{d}x' \gamma(t,x) D(x,x';t)\gamma(t,x'); \qquad \rho_1(t,x) = 0 \qquad (25) \\
&\text{II} : T_{n+1} \leq x < T_{n+1} + t_k \\
&\frac{\partial \phi(t,x)}{\partial t} = -\frac{\Lambda^{(2)}(t,x)}{2} + \rho_2(t,x) + \gamma(t,x)A(t,x) \qquad (26) \\
&\Lambda^{(2)}(t,x) = \Lambda_{n+1} = \int_{T_{n+1}}^{T_{n+2}} \mathrm{d}x' \gamma(t,x) D(x,x';t)\gamma(t,x');
\end{aligned}$$

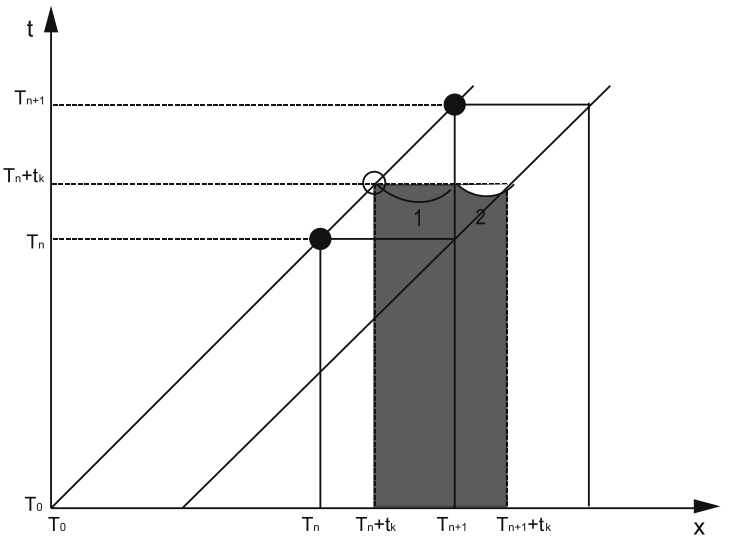

Fig. 8. The dependence of L_{nk} on the initial Libor $L(T_0, T_m)$, fixed at time T_0 from market data.

$$\rho_2(t,x) = \frac{e^{\phi_{n+1}(t)}\Lambda^{(2)}(t,x)}{1+e^{\phi_{n+1}(t)}}.$$

Eq. (25) represents the extension of LMM beyond the Libor lattice and Eq. (26) follows from the definition of drift given afore-time in Eq. (9). Fig. 7 shows the shaded portion, for which the drift $\Lambda^{(2)}$, ρ_2 is fixed by the drift given by Eq. (9); for the unshaded portion, the stochastic drift ρ_1 is zero but the deterministic drift $\Lambda^{(1)}$ is defined by extending the definition of drift beyond the Libor lattice.

The LMM has the initial condition specified at initial time T_0. The market fixes all $L(T_0, T_n)$ – and is shown in Fig. 8 – from which one can extract all the logarithmic rates $\phi(T_0, x)$. To express L_{nk} in terms of the initial condition one needs to integrate logarithmic rates $\phi(t, x)$ using Eqs. (25) and (26), namely

$$\begin{aligned}\int_{T_n+t_k}^{T_{n+1}+t_k}\phi(T_n+t_k,x)\mathrm{d}x = &\int_{T_n+t_k}^{T_{n+1}}\mathrm{d}x\left[\phi(T_0,x)+\int_{T_0}^{T_{n++}+t_k}\mathrm{d}t\left(-\frac{\Lambda^{(1)}(t,x)}{2}+\rho_1(t,x)+\gamma(t,x)A(t,x)\right)\right]\\ &+\int_{T_{n+1}}^{T_{n+1}+t_k}\mathrm{d}x\left[\phi(T_0,x)+\int_{T_0}^{T_{n++}+t_k}\mathrm{d}t\left(-\frac{\Lambda^{(2)}(t,x)}{2}+\rho_2(t,x)+\gamma(t,x)A(t,x)\right)\right].\end{aligned}$$

Note that the drifts for the two time intervals combine to yield

$$\begin{aligned}\Lambda^{(1)}(t,x)+\Lambda^{(2)}(t,x) &= \int_{T_n+t_k}^{T_{n+2}}\mathrm{d}x'\gamma(t,x)D(x,x';t)\gamma(t,x')\\ &\equiv \Lambda_{nk}(t,x).\end{aligned}$$

Hence, in terms of the initial values, Libor L_{nk} is given by

$$\begin{aligned}\ell L_{nk} &= e^{\int_{T_n+t_k}^{T_{n+1}+t_k}\phi(T_n+t_k,x)\mathrm{d}x} = e^{\int_{T_n+t_k}^{T_{n+1}+t_k}\phi(T_0,x)\mathrm{d}x-\frac{1}{2}q_{nk}^2+\varrho_{nk}+\omega_{nk}}\\ &= \ell L(T_0,T_n+t_k)\exp\left\{-\frac{1}{2}q_{nk}^2+\varrho_{nk}+\omega_{nk}\right\}\end{aligned}$$

where

$$\begin{aligned}q_{nk}^2 &= \int_{T_0}^{T_{n+1}+t_k}\mathrm{d}t\int_{T_n+t_k}^{T_{n+1}+t_k}\mathrm{d}x\Lambda_{nk}(t,x)\\ w_{nk} &= \int_{T_0}^{T_{n+1}+t_k}\mathrm{d}t\int_{T_n+t_k}^{T_{n+1}+t_k}\mathrm{d}x\gamma(t,x)A(t,x)\\ \varrho_{nk} &= \int_{T_0}^{T_{n+1}+t_k}\mathrm{d}t\int_{T_{n+1}}^{T_{n+1}+t_k}\mathrm{d}x\rho_2(t,x);\quad \rho_2(t,x)=\frac{e^{\phi_{n+1}(t)}}{1+e^{\phi_{n+1}(t)}}\Lambda_{n+1}(t,x).\end{aligned}\tag{27}$$

5. Approximate price of accrual swap

The term $\rho_2(t,x)$ in Eq. (26) makes L_{nk} depend nonlinearly on the quantum field $A(t,x)$. The volatility expansion for Libor drift was studied in Ref. [5]. One can expand L_{nk} as a power series in the volatility $\gamma(t,x)$, with the leading term yielding a linear theory for L_{nk}, and which in turn leads to an approximate analytic expression for the accrual swap.

The volatility approximation is based on the fact that $\rho_2(t,x) \approx \rho_2(T_0,x) + O(\gamma(t,x))$, and yields an expansion in $\phi(t) - \phi(T_0) = O(\gamma(t,x))$, which is a small quantity. Hence

$$\begin{aligned}\frac{e^{\phi(t)}}{1+e^{\phi(t)}} &= \frac{e^{\phi(T_0)}}{1+e^{\phi(T_0)}} + \frac{e^{\phi(t)} - e^{\phi(T_0)}}{(1+e^{\phi(t)})(1+e^{\phi(T_0)})} \\ &\simeq \frac{e^{\phi(T_0)}}{1+e^{\phi(T_0)}} + O(\gamma(t,x))\end{aligned} \tag{28}$$

and this leads to the following linearization

$$\begin{aligned}\ell L_{nk} &= e^{\int_{T_n+t_k}^{T_{n+1}+t_k} \phi(T_0,x)dx - \frac{1}{2}q_{nk}^2 + \varrho_{nk} + \omega_{nk}} \\ &\simeq \ell L(T_0, T_n+t_k) e^{-\frac{1}{2}q_{nk}^2 + \varrho_{nk}^0 + \omega_{nk}} + O(\gamma(t,x)).\end{aligned}$$

Collecting the deterministic terms, we have

$$L_{nk} \simeq L_{nk}^0 e^{\omega_{nk}}, \tag{29}$$

where

$$\begin{aligned}L_{nk}^0 &= L(T_0, T_n+t_k) e^{-\frac{1}{2}q_{nk}^2 + \varrho_{nk}^0} \\ \varrho_{nk}^0 &= \int_{T_0}^{T_{n+1}+t_k} dt \int_{T_{n+1}}^{T_{n+1}+t_k} dx \rho_2(T_0,x) \\ \rho_2(T_0,x) &= \frac{e^{\phi_{n+1}(T_0)}}{1+e^{\phi_{n+1}(T_0)}} \Lambda_{n+1}(T_0,x).\end{aligned}$$

The range condition can be rewritten by taking the logarithm of the limits and yields, from Eq. (29) the following:

$$a < L_{nk} < b \Rightarrow A \le \omega_{nk} \le B.$$

Hence, from Eq. (27)

$$A < \int_{T_0}^{T_n+t_k} dt \int_{T_n+t_k}^{T_n+t_k} dx \gamma(t,x) A(t,x) < B$$

where the logarithmic limits are given by

$$\begin{aligned}A &= \ln\left(\frac{a}{L_{nk}^0}\right) = \ln\left(\frac{a}{L(T_0,T_n)}\right) - \int_{T_0}^{T_n+t_k} dt \int_{T_{n+1}}^{T_{n+1}+t_k} dx \rho_2(T_0,x) + \frac{1}{2}q_{nk}^2; \\ B &= \ln\left(\frac{b}{L_{nk}^0}\right) = \ln\left(\frac{b}{L(T_0,T_n)}\right) - \int_{T_0}^{T_n+t_k} dt \int_{T_{n+1}}^{T_{n+1}+t_k} dx \rho_2(T_0,x) + \frac{1}{2}q_{nk}^2.\end{aligned}$$

The range function can be written using a delta function as follows:

$$1_{a<z<b} = \int_a^b \delta(\zeta - z) d\zeta = \frac{1}{2\pi} \int_a^b d\zeta \int e^{-i\xi(\zeta - z)} d\xi. \tag{30}$$

The expectation value of $1_{a<L_k^n<b}$ can be obtained in the framework of the path integral. The linear approximation for the drift reduces computing the expectation value to the evaluation of the following Gaussian path integral that, using Eq. (13), yields the following:

$$\begin{aligned}E_n[1_{a<L_{nk}<b}] &= \int_A^B d\zeta \int \frac{d\xi}{2\pi} e^{-i\xi\zeta} \frac{1}{Z} \int DA e^{S[A]} e^{i\xi \int_{T_n+t_k}^{T_{n+1}+t_k} dx \int_{T_0}^{T_n+t_k} dt \gamma(t,x) A(t,x)} \\ &= \int_A^B d\zeta \int \frac{d\xi}{2\pi} e^{-i\xi\zeta} e^{-\frac{1}{2}\xi^2 q_{nk}^2} = \int_A^B d\zeta \frac{1}{\sqrt{2\pi q_{nk}^2}} e^{-\frac{1}{2q_{nk}^2}\zeta^2} \\ &= N\left(\frac{B}{q_{nk}}\right) - N\left(\frac{A}{q_{nk}}\right); \qquad N(x) = \frac{1}{\sqrt{2\pi}} \int_{-\infty}^{z} dz e^{-\frac{1}{2}z^2}.\end{aligned}$$

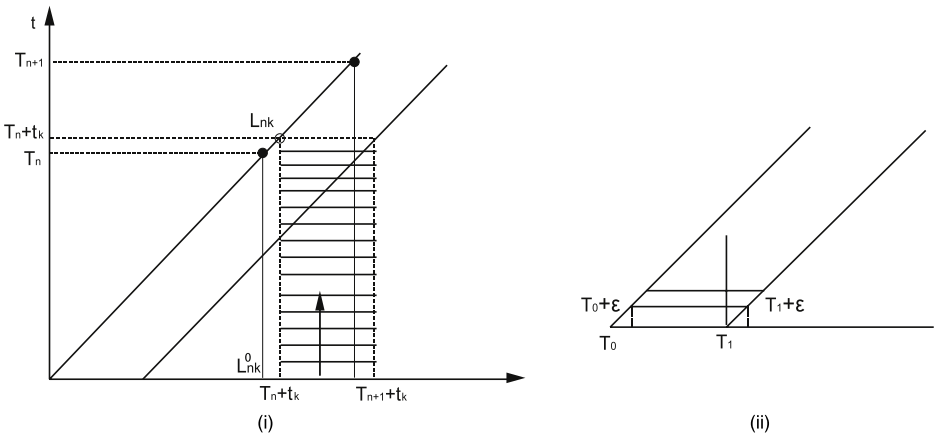

Fig. 9. The updating algorithm for obtaining sample values of L_{nk}.

The approximate price of the range accrual swaplet is given by

$$\text{Swaplet}_A(T_0, T_n; a, b) \simeq \ell VB(T_0, T_{n+1})\left\{L(T_0, T_n) - \frac{R_s}{M}\sum_{k=1}^{M}\left[N\left(\frac{B}{q_{nk}}\right) - N\left(\frac{A}{q_{nk}}\right)\right]\right\}. \tag{31}$$

The approximate price of the range accrual swap is given, from Eq. (23), by summing over the approximate price of each range accrual swaplet given in Eq. (31).

6. Simulation of range accrual swap

To evaluate the price of the accrual swap, one needs to generate sample values of the Libor L_{nk}. To do so one needs to start with the initial values of Libor $L(T_0, T_n)$, given by the market, and extract from the market Libor the initial value of the log-Libor rates $\phi(T_0, x)$ for all $T_0 \le x \le T_{N+1}$. The numerical algorithm is then used to generate the sample values of L_{nk}, as shown in Fig. 9, by simulating sample values of $\phi(t, x)$ with $t > 0$.

Suppose the present Libor interest rate is $\ell L(T_0, T_n) = \exp\{\int_{T_n}^{T_n+\ell} \mathrm{d}x\phi_0(T_0, x)\}$. At time T, where $T > T_0$, the log-Libor is given by

$$\phi(T, x) = \phi(T_0, x) + \int_{T_0}^{T} \mathrm{d}t\left\{-\frac{1}{2}\Lambda(t, x) + \rho(t, x) + \gamma(t, x)A(t, x)\right\}. \tag{32}$$

In the Monte Carlo simulation, the log-Libor rates $\phi(t, x)$ are updated on a discrete time lattice. Both calender time and future time are defined on a lattice with an interval of $\epsilon = 1$ day and yields

$$t \to t = T_0 + n\epsilon; \qquad x \to x = T_0 + m\epsilon. \tag{33}$$

The updating process for ϕ, from Eq. (32), is given by

$$\phi(t + \epsilon, x) = \phi(t, x) + \epsilon\left\{-\frac{1}{2}\Lambda(t, x) + \rho(t, x) + \gamma(t, x)A(t, x)\right\}. \tag{34}$$

Hence the updating process for Libor is given by

$$\begin{aligned}
\ell L(t + \epsilon, x) &= \exp\left\{\int_x^{x+\ell} \mathrm{d}x'\phi(t + \epsilon, x')\right\} \\
&= \exp\left\{\int_x^{x+\ell} \mathrm{d}x'\left[\phi(t, x') + \epsilon\left(-\frac{1}{2}\Lambda(t, x') + \rho(t, x') + \gamma(t, x')A(t, x')\right)\right]\right\} \\
&= \ell L(t, x)\exp\left\{\epsilon\int_x^{x+\ell} \mathrm{d}x'\left[-\frac{1}{2}\Lambda(t, x') + \rho(t, x') + \gamma(t, x')A(t, x')\right]\right\}.
\end{aligned}$$

As shown in Fig. 9(i), the value of $\phi(t, x)$ is updated in steps of ϵ, indicated by horizontal lines, until one generates the values of $\phi(T_n + T_k, x)$ required for obtaining a sample value of L_{nk}.

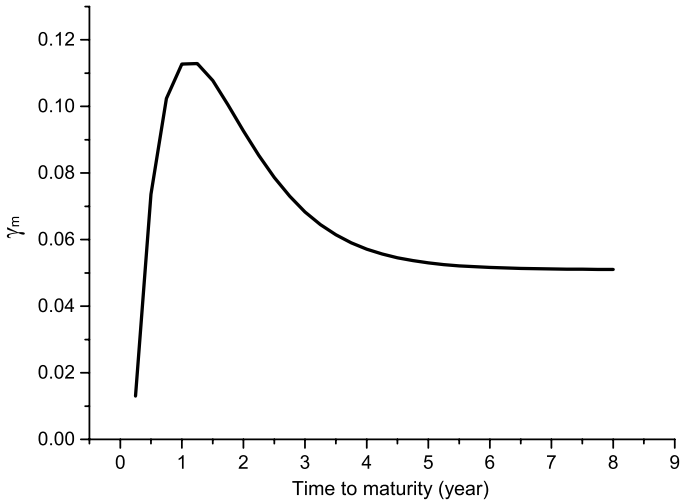

Fig. 10. Volatility $\gamma(x-t)$ of log-Libor field $\phi(t,x)$.

Libor volatility $\gamma_m(\theta)$, where $\theta = x - t$ is the time to maturity in the unit of year, is taken as an (empirical) input in the simulation. It is obtained from the formula of Baaquie and Yang [11] and is given below

$$\gamma_m(\theta) = 0.051 - 0.038\mathrm{e}^{-1.36*(\theta-0.25)} + 0.279(\theta - 0.25)\mathrm{e}^{-1.36*(\theta-0.25)}. \tag{35}$$

The volatility $\gamma_m(\theta)$ is plotted in Fig. 10.

The first updating generates sample values of L_{01}, with $T_0 + \epsilon = T_0 + t_1$, that is for $n = 0$, $k = 1$ and is shown in Fig. 9(ii). The algorithm yields

$$L_{01} = L(T_0+\epsilon, T_0+\epsilon) = L(T_0, T_0+\epsilon)\exp\left\{\epsilon\int_{T_0+\epsilon}^{T_1+\epsilon} \mathrm{d}x\Big[-\frac{1}{2}\Lambda(T_0,x) + \rho(T_0,x) + \gamma(T_0,x)A(T_0,x)\Big]\right\}.$$

The range of $T_0 + \epsilon \le x < T_1 + \epsilon$ cuts across the Libor lattice at T_1, as shown in Fig. 9(ii). The drift, from Eqs. (25) and (26), has the following definition:

$$\mathrm{I} : T_0 + \epsilon \le x < T_1; \quad T \equiv T_0 + \epsilon$$

$$\Lambda(T,x) = \Lambda^{(1)}(T,x) = \int_{T_0+\epsilon}^{T_1} \mathrm{d}x'\gamma(T,x)D(x,x';T)\gamma(T,x')$$

$$\rho(T,x) = \rho_1(T,x) = 0$$

$$\mathrm{II} : T_1 \le x < T_1 + \epsilon$$

$$\Lambda(T,x) = \Lambda^{(2)}(T,x) = \int_{T_1}^{T_2} \mathrm{d}x'\gamma(T,x)D(x,x';t)\gamma(T,x');$$

$$\rho(T,x) = \rho_2(T,x) = \frac{\mathrm{e}^{\phi_1(T_0)}\Lambda^{(2)}(T_0,x)}{1+\mathrm{e}^{\phi_1(T_0)}}.$$

Fig. 11 shows a typical configuration for Libor L_{nk} generated by our simulation. The value for volatility was taken to be $50 \times \gamma_m$ – where γ_m is the market volatility of Libor L_{nk} – to magnify the effect of the barrier crossings.

In the simulation, the price of the accrual swaplet is obtained by evaluating the average of the payoff for the sample configurations and yields

$$\mathrm{Swaplet}_A(T_0,T_n;a,b) = \ell VB(T_0,T_{n+1})\left\{L(T_0,T_n) - \frac{R_s}{M}\sum_{k=1}^{M}\frac{1}{\mathcal{N}}\sum_{l=1}^{\mathcal{N}}[1_{a\le L_{nk}^{(l)}\le b}]\right\}$$

where $L_{nk}^{(l)}$ are the sample values of Libor and $\mathcal{N}$ is the total number of sample configurations.

7. Result and discussion

The starting date T_0 is 0, and T_1 is set to be 90 days for the first settlement. The initial 90-day Libor at T_0 is $L(T_0,T_0) = 0.0269$ and the range we set is (0.020, 0.030); In the simulation, $\epsilon = 1$ day .

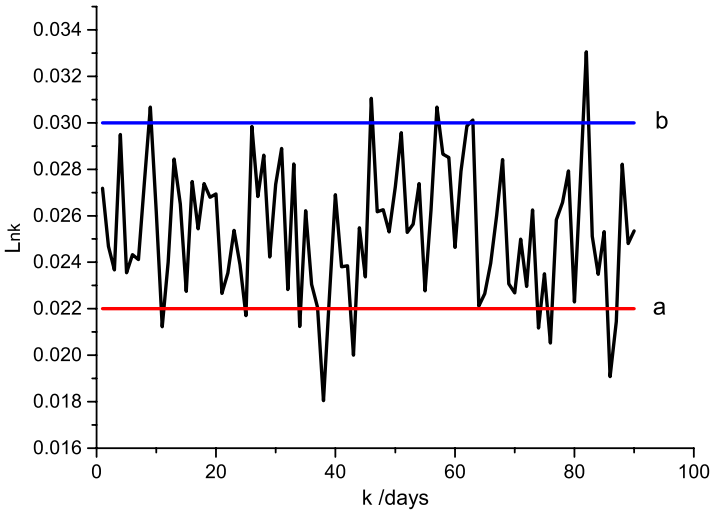

Fig. 11. A sample configuration of Libor L_{nk} for volatility $\gamma = 50 * \gamma_m$.

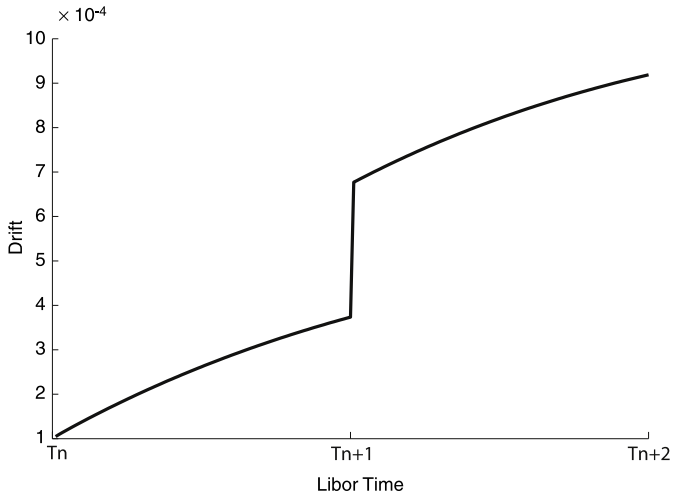

Fig. 12. The discontinuity of drift across the Libor lattice at T_{n+1}.

Fig. 12 shows the jump in the drift across a Libor lattice time. This is to be expected since on the diagonal edge, for a swaplet$(T_n, T_n; a, b)$, the drift for $x < T_{n+1}$ is deterministic whereas the drift for $x < T_{n+1}$ is a sum of deterministic and stochastic terms.

Define $I(k) = E_n[1_{a<L_{nk}<b}]$ to be the average value of Libor L_{nk} being in the range $[a, b]$ on kth day for numeraire $B(t, T_{n+1})$; we compute

$$\text{Approximate: } I_G(k) = N\left(\frac{B}{q_{nk}}\right) - N\left(\frac{A}{q_{nk}}\right)$$

$$\text{Simulation: } I_S(k) = \frac{1}{\mathcal{N}}\sum_{l=1}^{\mathcal{N}}[1_{a\le L_{nk}^{(l)}\le b}].$$

The simulated value of $I(k)$ is compared with the approximation.

As shown in Fig. 13, the approximate price is exactly the same with the simulation result when $\gamma = \gamma_m$. However it has a slight difference when $\gamma = 25 * \gamma_m$ but still can be acceptable in practice with the absolute error under 2%. The approximate result tends to have large errors with simulation when $\gamma = 50 * \gamma_m$ and $\gamma = 100 * \gamma_m$.

Define

$$\text{Absolute error} = \frac{1}{M}\sum_{k=1}^{M}\frac{|I_G(k) - I_S(k)|}{I_S(k)}.$$

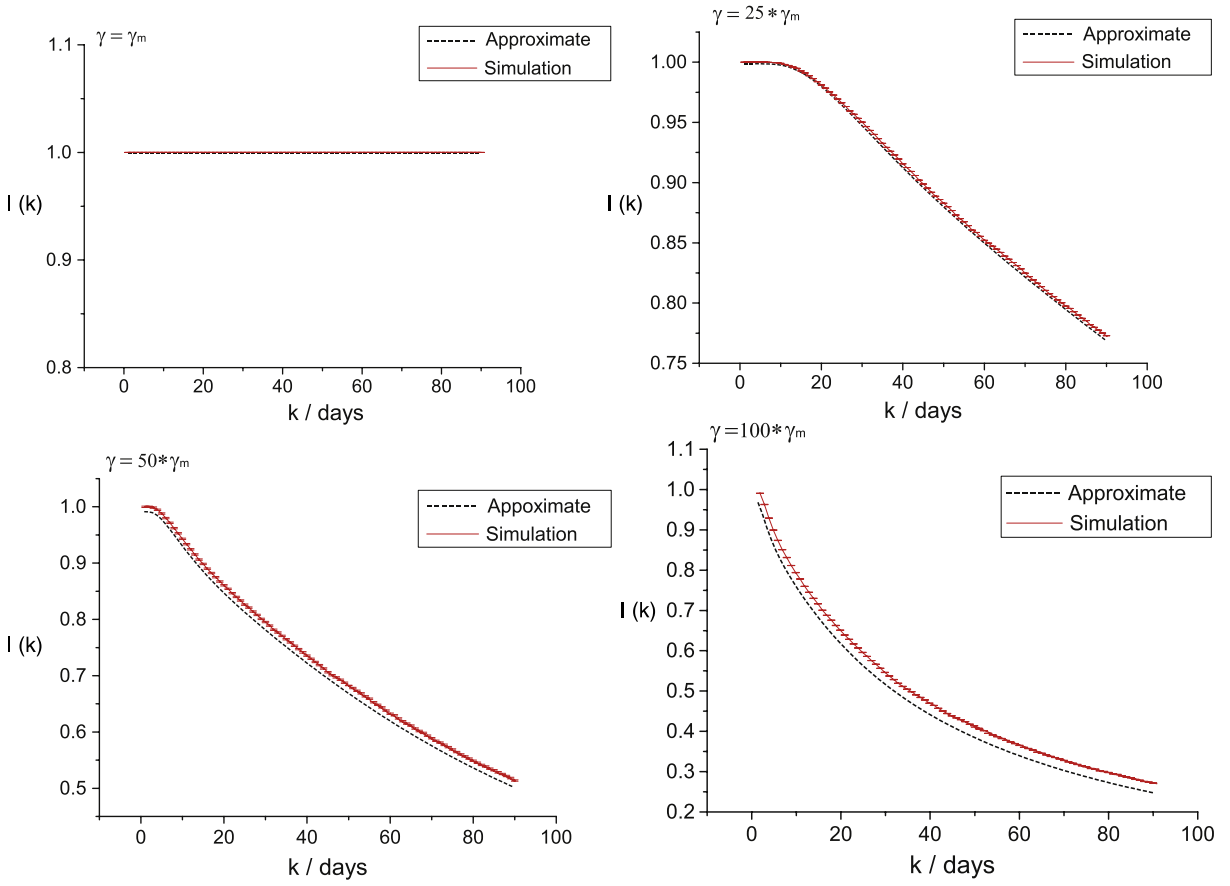

Fig. 13. Comparison between simulation and approximate values of $I(k)$. The error bars are Monte Carlo errors of the simulation. The bound range is set 0.022–0.030.

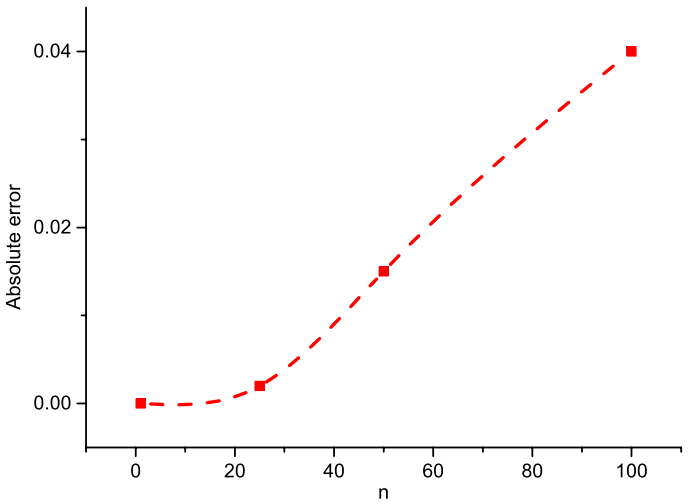

Fig. 14. Absolute errors on times of volatilities $\gamma = n * \gamma_m$.

The absolute errors for different magnitudes of volatility are shown Fig. 14. The approximation fails to give an accurate for volatility greater than $\gamma = 25 * \gamma_m$, as expected.

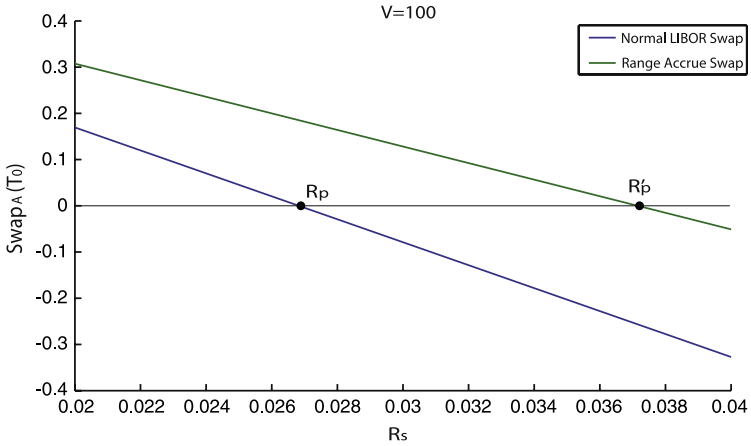

Fig. 15. Par value of the normal and accrual swap, given by $\text{Swap}(R_p, T_0) = 0 = \text{Swap}_A(R'_p, T_0)$, respectively.

The accrual swap price as a function of fixed leg R_S is plotted in Fig. 15. The par value of accrual swap R'_p shows a larger value compared to the normal interest rate swap R_P. The par value shows the utility of the accrual swap, since one is effectively paying a much smaller value for the floating leg if the market becomes very volatile; and hence, in effect, one is receiving a higher fixed leg if the market is very volatile.

8. Conclusion

The objective of this study was to price the interest rate range accrual swaps based on the formalism of quantum finance. The definition of the payoff function for the accrual swap required the employment of the logarithmic interest rates given by $\phi(t, x)$. The Libor Market Model defined for the Libor lattice was extended to accommodate the payoff of the accrual swap and this in turn was only possible because the pricing was obtained using the logarithmic field $\phi(t, x)$: unlike Libor $L(T, T_n)$, which is only defined for the Libor lattice, $\phi(t, x)$ is defined for the continuous domain defined by $t \geq T_0, x \geq t$.

An approximate formula was obtained by linearizing the nonlinear drift of the LMM. The Libor rates were studied numerically by using a simulation for updating daily Libor. The simulation showed that the approximate price provides an excellent approximation when the Libor volatility γ_m is taken from the market. The simulation showed that the approximate accrual swap formula fails only for very high volatility that one does not expect for normal market conditions. The par value of the range accrual swap can be computed accurately using the approximate formula and opens the way for empirically studying the pricing of range accrual swaps.

Acknowledgment

The authors thank Jitendra D. Bhanap for many useful discussions.

Appendix A. Derivation of the drift

LMM drift $\rho(t, x)$ above is derived based directly on the LMM Hamiltonian. We choose $B(t, T_{l+1})$ to be the forward bond numeraire; for all n, the drift is fixed so that $\chi_n(t) \equiv \frac{B(t,T_{n+1})}{B(t,T_{l+1})}$ is a martingale. The drift $\rho(t, x)$ is determined in the Hamiltonian framework by the following condition [5]:

$$\mathcal{H}_\phi(t)\chi_n(t) = \mathcal{H}_\phi(t)\Big[\frac{B(t, T_{n+1})}{B(t, T_{l+1})}\Big] = 0 : \text{ for all } n. \tag{36}$$

Recall $\ell L(t, T_n) = \exp\{\int_{T_n}^{T_{n+1}} \mathrm{d}x\phi(t, x)\} \equiv \mathrm{e}^{\phi_n}$. The Hamiltonian of the Libor Market Model given by Baaquie [5],

$$\mathcal{H}_\phi(t) = -\frac{1}{2}\int_{x,x'} M_\gamma(x, x'; t)\frac{\delta^2}{\delta\phi(x)\phi(x')} + \frac{1}{2}\int_x \Lambda(t, x)\frac{\delta}{\delta\phi(x)} - \int_x \rho(t, x)\frac{\delta}{\delta\phi(x)}$$

$\rho(t, x) = \sum_{n=0}^{\infty} \theta_n(x)\rho_n(t, x)$; $\Lambda(t, x) = \sum_{n=0}^{\infty} \theta_n(x) \int_{T_n}^{T_{n+1}} \mathrm{d}x' M_\gamma(x, x'; t)$

where $\theta_k(x)$ has the value 1 in the Libor range $T_k \leq x < T_{k+1}$ and is equal to 0 when out of the range.

Functional differentiation by $\phi(x)$ yields $\frac{\delta L(t,T_k)}{\delta\phi(x)} = \theta_k(x)L(t, T_k)$. The following are the three cases for the derivation.

Case (i) $n > I$, $\chi_n(t) = \prod_{k=I+1}^{n} \frac{1}{1+\ell L(t,T_k)} = \exp\{-\sum_{k=I+1}^{n} \ln(1+\ell L(t,T_k))\}$

$$\frac{\delta \chi_n(t)}{\delta \phi(x)} = -\sum_{k=I+1}^{n} \frac{e^{\phi_k}\theta_k(x)}{1+e^{\phi_k}}. \tag{37}$$

The summation term above is due to the discounting by the forward numeraire $B(t, T_{I+1})$. The second derivative yields

$$\frac{\delta^2 \chi_n(t)}{\delta\phi(x)\delta\phi(x')} = -\sum_{k=I+1}^{n}\left(\frac{e^{\phi_k}}{1+e^{\phi_k}}\right)^2 \theta_k(x)\theta_k(x') - \sum_{k=I+1}^{n}\frac{e^{\phi_k}\theta_k(x)\theta_k(x')}{1+e^{\phi_k}} + \sum_{j,k=I+1}^{n}\frac{e^{\phi_j+\phi_k}\theta_k(x)\theta_k(x')}{(1+e^{\phi_j})(1+e^{\phi_k})}.$$

Applying the log Libor Hamiltonian on $\chi_n(t)$

$$\begin{aligned}\mathcal{H}_\phi \chi_n(t) = \frac{1}{2}\int_{x,x'} M_\gamma \Bigg[&\sum_{k=I+1}^{n}\left(\frac{e^{\phi_k}}{1+e^{\phi_k}}\right)^2 \theta_k(x)\theta_k(x') - \sum_{j,k=I+1}^{n}\frac{e^{\phi_j+\phi_k}\theta_k(x)\theta_j(x')}{(1+e^{\phi_j})(1+e^{\phi_k})} \\ &+ \sum_{k=I+1}^{n}\frac{e^{\phi_k}\theta_k(x)\theta_k(x')}{1+e^{\phi_k}}\Bigg] - \frac{1}{2}\int_{x,x'} M_\gamma \sum_{n=0}^{\infty}\theta_n(x)\sum_{k=I+1}^{n}\frac{e^{\phi_k}\theta_k(x')}{1+e^{\phi_k}} + \int_x \rho(t,x)\sum_{k=I+1}^{n}\frac{e^{\phi_k}\theta_k(x)}{1+e^{\phi_k}}.\end{aligned}$$

Note the remarkable identity

$$\frac{1}{2}\sum_{j,k=I+1}^{n} A_{jk} = \sum_{j=I+1}^{n}\sum_{k=I+1}^{j} A_{jk} - \frac{1}{2}\sum_{k=I+1}^{n} A_{kk}.$$

Taking

$$A_{jk} = \frac{e^{\phi_j+\phi_k}\theta_k(x)\theta_j(x')}{(1+e^{\phi_j})(1+e^{\phi_k})}$$

yields, after some cancelations

$$\mathcal{H}_\phi \chi_n(t) = \int_x \rho(t,x)\sum_{k=I+1}^{n}\frac{e^{\phi_k}\theta_k(x)}{1+e^{\phi_k}} - \int_{x,x'} M_\gamma \sum_{j=I+1}^{n}\sum_{k=I+1}^{j}\frac{e^{\phi_j+\phi_k}\theta_k(x)\theta_j(x')}{(1+e^{\phi_j})(1+e^{\phi_k})} \tag{38}$$

and the Libor drift is given by

$$\begin{aligned}\rho_n(t,x) &= \sum_{j=I+1}^{n}\frac{e^{\phi_j}}{1+e^{\phi_j}}\int_{x'} M_\gamma(x,x';t) \\ &= \sum_{j=I+1}^{n}\frac{e^{\phi_j}}{1+e^{\phi_j}}\Lambda_j(x); \quad T_n \le x < T_{n+1}\end{aligned}$$

applied to Eq. (38) leads to the cancelation of all the terms and yields the final result

$$\mathcal{H}_\phi \chi_n(t) = 0: \text{ martingale.} \tag{39}$$

Case (ii) $n < I$, the derivation is similar to Case (i)

$$\chi_n(t) = \prod_{k=n+1}^{I}(1+\ell L(t,T_k)) = \exp\left\{\sum_{k=n+1}^{I}\ln(1+\ell L(t,T_k))\right\}$$

$$\Rightarrow \rho_n(t,x) = -\sum_{j=n+1}^{I}\frac{e^{\phi_j}}{1+e^{\phi_j}}\Lambda_j(x); \qquad T_n \le x < T_{n+1}.$$

Case (iii) $n = I$, $\chi_n(t) = 1$ yields $\mathcal{H}_\phi \chi_I(t) = 0 \Rightarrow \rho_I(t,x) = 0$.

Appendix B. Simulation of the quantum field $A(t,x)$

Assume that $D(x,x';t) = D(\theta,\theta')$ for the remaining future time $\theta = x - t$, $\theta' = x' - t$. The propagator

$$E[A(t,x)A(t',x')] = \delta(t-t')D(\theta,\theta')$$

is the defining equation for simulating a Gaussian quantum field $A(t,x)$. Because the propagator (correlation function) D is always a positive and symmetric matrix, Cholesky decomposition can be used for decomposing D into the product of a lower triangular matrix and its conjugate transpose.

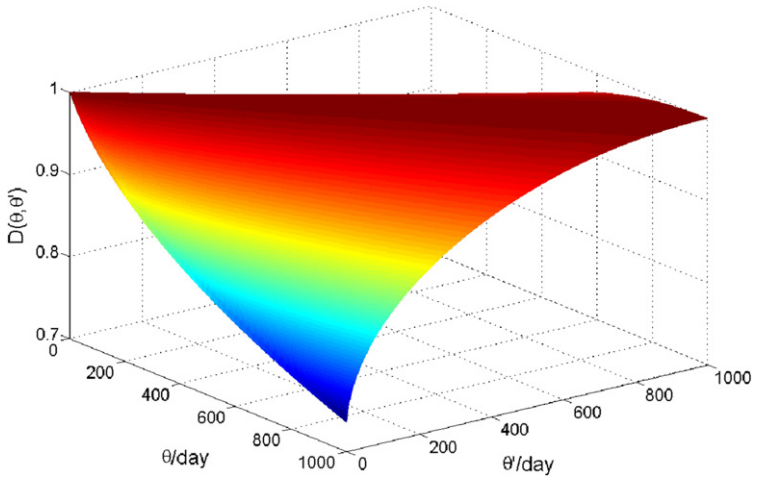

Fig. 16. Propagator $D(\theta, \theta')$.

The propagator used for the simulation is given in Ref. [11]

$$D(\theta, \theta') = \frac{\lambda}{2\sinh(2b)}[g(\theta + \theta') + g(\theta - \theta')] \tag{40}$$

$$g(\theta) = \mathrm{e}^{-\lambda|\theta|\cosh(b)} \sinh\{b + \lambda|\theta|\cosh(b)\} \tag{41}$$

where $\lambda = \widetilde{\lambda}^{\eta}$, the calibration parameters are $\widetilde{\lambda} = 1.79$, $b = 0.85$, $\eta = 0.34$. The normalized propagator is plotted in Fig. 16.

Let $0 \leq \theta \leq \theta_M$, where $\theta_M = T - t$; the Cholesky decomposition for the propagator [12] yields

$$D(\theta, \theta') = \int_0^{\theta_M} Y(\theta, \zeta) Y^T(\zeta, \theta') \mathrm{d}\zeta.$$

For $\theta = T - t$, let

$$A(t, x) = \int \mathrm{d}\zeta\, Y(\theta, \zeta) R(t, \zeta)$$

where $E[R(t, \zeta)R(t', \zeta')] = \delta(t - t')\delta(\zeta - \zeta')$. $R(t, \zeta)$ is an independent Gaussian random variable for each calendar time t and future remaining time ζ. The simulation requires discrete calendar time and future time. For infinitesimals ϵ_t, ϵ_x we have

$$t, x \to m\epsilon_t, n\epsilon_x; \quad \theta \to p = m - n.$$

The quantum field $A(t, x)$ and log-Libor rates $\phi(t, x)$ are expressed by

$$A(t, x) \to A_{m,n}; \qquad \phi(t, x) \to \phi_{m,n}.$$

For the process of updating $\phi_{m,n}$, the step size of calendar time t and the step size of future time x are also chosen to be equal $\epsilon = \epsilon_t = \epsilon_x = 1$ day,

$$\phi_{m+1,n} = \phi_{m,n} + \epsilon(\rho_{m,n} + \gamma_{m,n} A_{m,n}).$$

The remaining future times $\theta = p$ and $\theta = p'$ in discrete time, are $p = n - m$ and $p' = n' - m'$ respectively.

$$E[A_{m,n} A_{m',n'}] = \frac{\delta_{m-m'}}{\epsilon} D[(n - m)\epsilon, (n' - m')\epsilon] = \frac{\delta_{m-m'}}{\epsilon} D_{p,p'}.$$

Then

$$D_{p,p'} = \sum_{q=0}^{M-n} Y_{p,q} Y_{q,p'}; \qquad A_{m,n} = \sum_{p'=0}^{M-n} Y_{p,p'} R_{m,p'}$$

where, for normal random variables R_{mn} are all identical and

$$R_{mn} = \frac{1}{\sqrt{\epsilon}} N(0, 1). \tag{42}$$

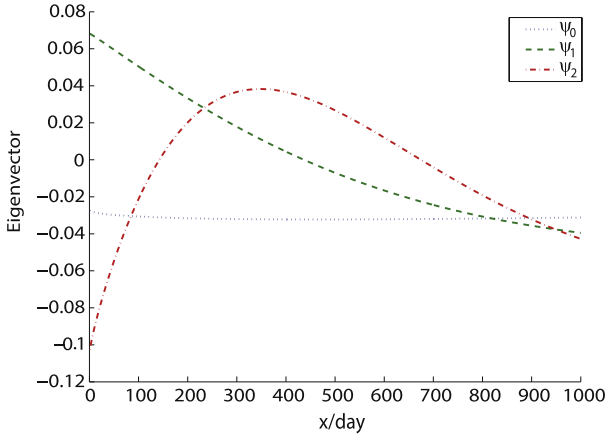

(a) Eigenvector.

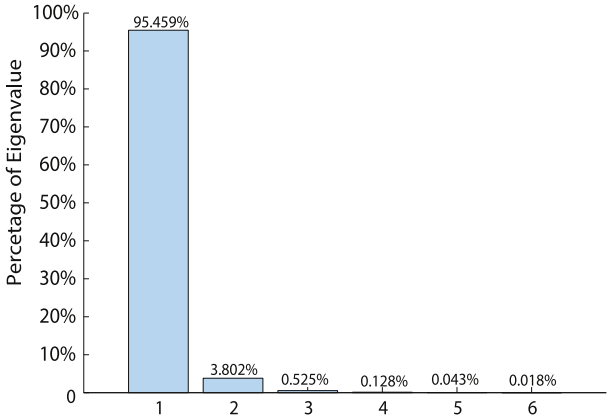

(b) Eigenvalue.

Fig. 17. The eigenvector and eigenvalue for the ground state, first excited state and second excited state.

The drift term $\rho_{m,n}$ in discrete time is given by

$$\rho_{m,n} = \epsilon\gamma_p \sum_{p=M_*-m}^{M-n} D_{p,p'}\gamma'_p.$$

The eigenvalues and eigenvectors of the stiff propagator are

$$\sum_{p'=0}^{M-n} D_{p,p'}\psi_\iota(p') = \lambda_\iota\psi_\iota(p); \quad \iota = 0, 1, 2 \ldots M-n$$

where λ_ι is the eigenvalue of propagator D and ψ_ι its eigenvector. Note that

$$\sum_{\iota=0}^{M-n} \psi^*_\iota(p)\psi_\iota(p') = \delta_{p-p'}.$$

Hence

$$A_{m,n} = \sum_{p'=0}^{M-n} Y_{p,p'}R_{m,p'} = \sum_{\iota=0}^{M-n} \sqrt{\lambda_\iota}\psi_\iota(p)Q_{m,l}$$

$$Y_{p,p'} = \sum_{\iota=0}^{M-n} \sqrt{\lambda_\iota}\psi^*_\iota(p)\psi_\iota(p'); \qquad Q_{m,l} = \sum_{p'=0}^{M-n} \sqrt{\lambda_\iota}\psi_\iota(p')R_{m,p'}.$$

The first eigenvalue is nearly 96% of the sum of eigenvalues, 3% and 0.4% are accounted for by the second and third eigenvalues, respectively. This fact suggests that three eigenvalues are enough for constructing the structure of the propagator as shown in Fig. 17.

$$\begin{aligned}\phi_{m+1,n} &= \phi_{m,n} + \epsilon(\rho_{m,n} + \gamma_{m,n}A_{m,n}) \\ &= \phi_{m,n} + \epsilon\rho_{m,n} + \epsilon\gamma_{m,n}\sum_{\iota=0}^{M-n}\sqrt{\lambda_\iota}\psi_\iota(p)Q_{m,l} \\ &= \phi_{m,n} + \epsilon\rho_{m,n} + \epsilon\sum_{\iota=0}^{M-n}\gamma^l_{m,n}\sqrt{\lambda_\iota}\psi_\iota(p)Q_{m,l}\end{aligned}$$

$\gamma^l_{m,n} = \gamma_{m,n}\sqrt{\lambda_\iota}\psi_\iota(p)$ is the effective volatility.

References

[1] Patrick Navatte, François Quittard-Pinon, The valuation of interest rate digital options and range notes revisited, Eur. Financ. Manage. 5 (3) (1999) 425–440.
[2] João Pedro Vidal Nunes, Multifactor valuation of floating range notes, Math. Finance 14 (1) (2004) 79–97.
[3] Damiano Brigo, Fabio Mercurio, Interest Rate Models—Theory and Practice: with Smile, Inflation and Credit, Springer, 2006.
[4] Bong-Gyu Jang, Ji Hee Yoon, Analytic valuation formulas for range notes and an affine term structure model with jump risks, J. Banking Finance 34 (9) (2010) 2132–2145.
[5] Belal E. Baaquie, Interest Rates and Coupon Bonds in Quantum Finance, Cambridge University Press, 2009.
[6] L.P. Kadanoff, Kenneth Geddes Wilson (1936–2013) nobel-prize winning physicist who revolutionized theoretical science, Nature 500 (7460) (2013) 30.
[7] Edward Witten, Quantum field theory and the jones polynomial, Comm. Math. Phys. 121 (3) (1989) 351–399.
[8] E. Haven, A. Khrennikov, Quantum Social Science, Cambridge University Press, UK, 2013.
[9] B.E. Baaquie, Financial modeling and quantum mathematics, Comput. Math. Appl. 65 (2013) 1665–1673.
[10] Belal E. Baaquie, Quantum Finance, Cambridge University Press, UK, 2004.
[11] Belal E. Baaquie, Yang Cao, Empirical analysis of quantum finance interest rates models, Physica A 388 (13) (2009) 2666–2681.
[12] Belal E. Baaquie, Pan Tang, Simulation of nonlinear interest rates in quantum finance: libor market model, Physica A 391 (4) (2012) 1287–1308.